

# Fuzzy Logic Control Of Mosfet Inverter Grid-Tied Photovoltaic System

#1 D. Narasimhulu #2 Er. P. Pedda Reddy

#1 Pursuing M.tech, #2 Assistant professor, Department of EEE

St. Johns College of Engineering & Technology, Yerrakota, Yemmiganur, Kurnool, Andhra Pradesh.

**Abstract:** Proposes a cost effective solar power generation in grid arrangement in a resourceful approach. The photovoltaic systems consist of two converter stations between PV array and to the utility. It composed of transformer less inverter controlled by the fuzzy logic controller. The power generated from the solar panel improved by the boost converter that are connected next to the solar panel. For the transfer of DC to AC, the power generated from the solar panel DC and that are converted to AC by means of single phase inverter which generate AC output. However, the MOSFETs are limited to use in transformer less PV inverter due to the low reverse recovery characteristics of the body diode. In this paper, a family of new transformer less PV inverter topology for single-phase grid-tied operation is proposed using super-junction MOSFETs and Sic diodes as no reverse recovery issues are required for the main power switches for unity power operation. The added clamping branch clamps the freewheeling voltage at the half of dc input voltage during the freewheeling period. Results showed a low current distortion at output.

**Index Terms—**Common-mode (CM) voltage, converter, European efficiency, grid connected, high efficiency, leakage current, photovoltaic (PV), fuzzy logic.

## I. INTRODUCTION:

Transformer less inverters are widely used in grid-tied photovoltaic (PV) generation systems, due to the benefits of achieving high efficiency and low cost. Various transformer less inverter topologies have been proposed to meet the safety requirement of leakage currents, when no transformer is used in a grid connected photovoltaic system, a galvanic connection between the grid and PV array exists. In these conditions, dangerous leakage currents (common-mode currents) can appear through the stray capacitance between the PV array and the ground. In order to avoid these leakage currents, different inverter topologies that generate no varying common-mode voltages have been proposed.

## II. VARIOUS TRANSFORMERLESS TOPOLOGIES

In recent years, there have been quite a few new transformerless PV inverters topologies, which eliminate traditional line frequency transformers to achieve lower cost and higher efficiency, and maintain lower leakage current as well. One unipolar inverter topology, H5, as shown in Fig.1, solves the ground leakage current issue and uses hybrid MOSFET and IGBT devices to achieve high efficiency.

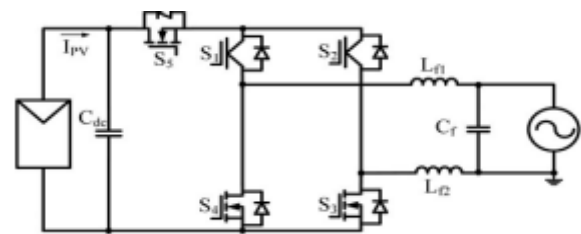


Fig.1. H5 Topology

This topology has high conduction losses due to the fact that the current must conduct through three switches in series during the active phase. Another disadvantage of the H5 is that the line-frequency switches S1 and S2 cannot utilize MOSFET devices because of the MOSFET body diode's slow reverse recovery. The slow reverse recovery of the MOSFET body diode can induce large turn-on losses, has a higher possibility of damage to the devices and leads to EMI problems. Shoot-through issues associated with traditional full bridge PWM inverters remain in the H5 topology due to the fact that the three active switches are series-connected to the dc bus.

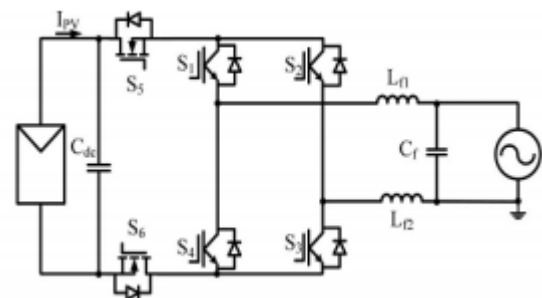


Fig.2. H6 Topology

H6 Topology uses MOSFETs to decrease the conduction loss of IGBTs in H5 topology, by splitting S5 of H5 topology into two MOSFETs i.e. S5 and S6 in series and operates them in high-frequency switching, S1–S4 in line grid line frequency switching. Uency switching, S1–S4 in line grid line frequency switching. Drawbacks of this inverter are higher conduction loss from four devices in conduction loop

### III. PROPOSED TOPOLOGY

The family of the proposed transformer less PV inverter topology is depicted in Fig. 3 which is derived according to the derivation method described in the prior section, where S1, S2, S4, and S5 are high-frequency switches, and S3 and S6 are low frequency freewheeling switches. The unidirectional clamping branch is constructed using switch S7 and diode D3 with a capacitor divider (Cdc1 and Cdc2) which clamps the CM voltage at the midpoint of dc link. LA, LB, and Co make up the LC type filter connected to the grid and Vpv represent the input dc voltage. The unipolar SPWM can be employed to the proposed topology with three-level output voltage. The MOSFET power switches are utilized as no reverse-recovery issues are required for the proposed configuration of the inverter for unity power factor operation. Consequently, the efficiency of the entire PV system is increased.

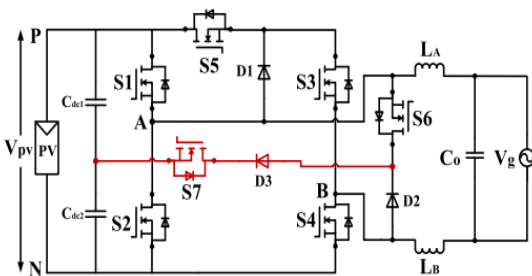


Fig 3 proposed transformer less grid-connected PV inverter structure

#### 3.1 Operating principle

In order to analyse and verify, the circuit structure (a) is taken as an example, it shows the switching pattern for unity power factor operation, where the G1, G2, G3, G4, G5, G6 and G7 are the gate signals of the switches S1, S2, S3, S4, S5, S6 and S7. As can be seen, (S1, S4) and (S2, S5) commute at the switching frequency with the identical commutation order in the positive and negative half cycle of the grid current, respectively. The operating principles of the proposed topology are shown. Four operation modes are proposed to generate the output voltage stste of +Vpv, 0 and -Vpv, which can explained as follows

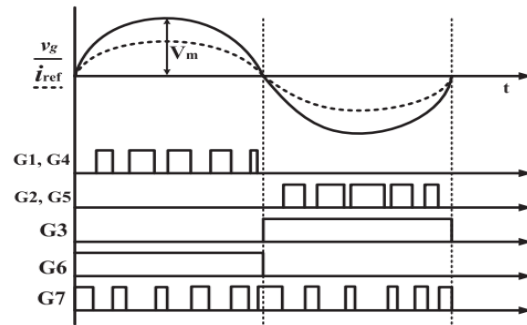


Fig 4 Gate drive signals of the proposed topology

1) Mode 1 is the active in the positive half cycle of the grid current. When S1, S4 are turned-on, the inductor current  $i_L$  increases linearly through grid. In this mode,  $V_{AN} = V_{PV}$  and  $V_{BN} = 0$ , thus  $V_{AB} = V_{PV}$  and the inductor current:  $i_L = V_{pv} - V_g / L(t)$

2) Mode 2 is the freewheeling mode in the positive half cycle of the grid current. The inductor current  $i_L$  flows through S6 and D2, and reduces linearly under the effect of grid voltage. In this state,  $V_{AN}$  falls and  $V_{BN}$  rises until their values are equal. If the voltages ( $V_{AN} \sim V_{BN}$ ) are higher than half of the dc link voltage, freewheeling current flows through S7 & D3 to the midpoint of the dc link, results  $V_{AN}$  and  $V_{BN}$  are clamped at  $V_{PV}/2$ . Therefore, at mode 2,  $V_{AN} = V_{PV}/2$ ,  $V_{BN} = V_{PV}/2$ , the inverter output voltage  $V_{AB} = 0$  and the inductor current:  $i_L = -V_g / L(t)$

3) Mode 3 is the active mode in the negative half cycle of grid current. Similar to mode 1, when S2, S3, and S5 are turned-on, the voltage  $V_{AN} = 0$  and  $V_{BN} = V_{PV}$ , thus  $V_{AB} = -V_{PV}$  and the inductor current:  $i_L = V_{pv} - V_g / L(t)$

4) Mode 4 is the freewheeling mode in the negative half cycle of grid current. When S5 and S2 are turned-off, the inductor current flows through S3 and D1. Similar to mode 2, if the voltages ( $V_{AN} = V_{BN}$ ) are higher than half of the dc link voltage, freewheeling current flows through S7 and D3 to the mid-point of the dc link, results the voltages  $V_{AN}$  and  $V_{BN}$  are clamped at  $V_{PV}/2$ . Therefore, in this mode,  $V_{AB} = 0$ , and the inductor current:  $i_L = -V_g / L(t)$  As described above, the freewheeling path potential is clamped at the mid-point of the dc link during freewheeling period of positive and negative half cycle. As a result, the scene that the anti-parallel diodes of the MOSFETs remained inactive during the whole grid operation period. Therefore, the proposed could be implemented utilizing MOSFET switches. However, the body-diode will be activated if a phase shift is occurred in the inverter output voltage and current. Accordingly, the dependability of the system will be reduced because of the MOSFET anti-parallel diode low reverse recovery issues.

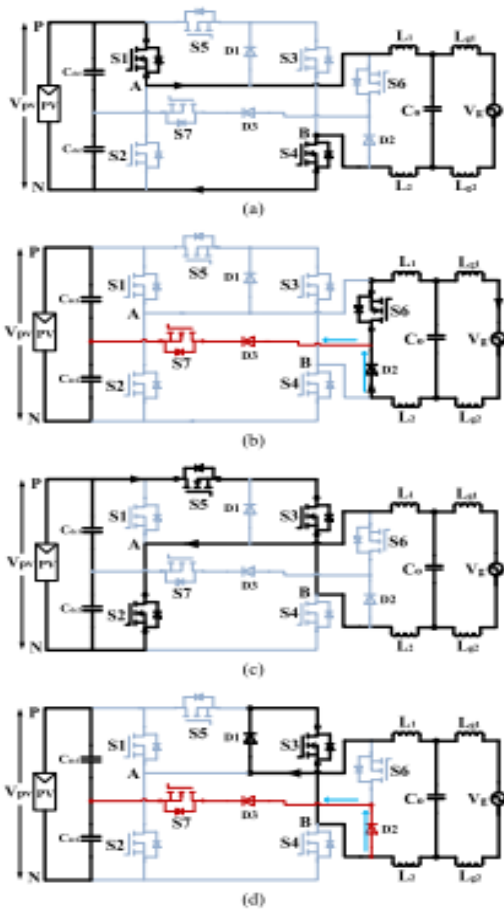


Fig. 5. Operating principle of the proposed topology: (a) Active and (b) freewheeling modes in the positive half cycle of the grid current, (c) active and (d) freewheeling modes in the negative half cycle of the grid current.

#### IV. FUZZY LOGIC

In recent years, the number and variety of applications of fuzzy logic have increased significantly. The applications range from consumer products such as cameras, camcorders, washing machines, and microwave ovens to industrial process control, medical instrumentation, decision-support systems, and portfolio selection. To understand why use of fuzzy logic has grown, you must first understand what is meant by fuzzy logic.

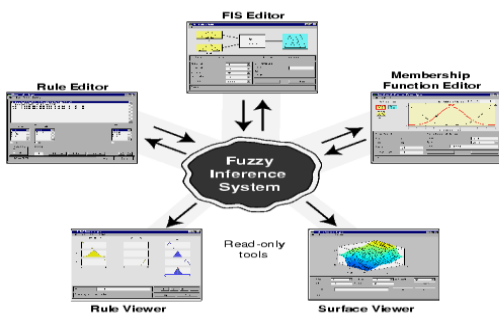


Fig.6 The Primary GUI Tools Of The Fuzzy Logic Toolbox

The FIS Editor handles the high level issues for the system How much input and output variables? What are their names? The Fuzzy Logic Toolbox doesn't limit the number of inputs. However, the number of inputs may be limited by the available memory of our machine. If the number of inputs is too large, or the number of membership functions is too big, then it may also be difficult to analyse the FIS using the other GUI tools. The Membership Function Editor is used to define the shapes of all the membership functions associated with each variable. The Rule Editor is for editing the list of rules that defines the behaviour of the system.

#### 4.1 The FIS Editor

The following discussion walks we through building a new fuzzy inference system from scratch. If we want to save time and follow along quickly, we can load the already built system by typing fuzzy tipper This will load the FIS associated with the file tipper. Is (the .fis is implied) and launch the FIS Editor. However, if we load the pre-built system, we will not be building rules and constructing membership functions.

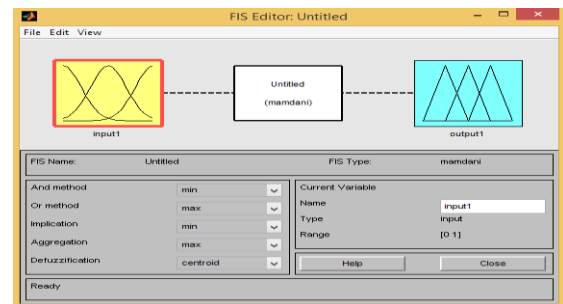


Fig.7 The FIS Editor

We will see the diagram updated to reflect the new names of the input and output variables. There is now a new variable in the workspace called tipper that contains all the information about this system.

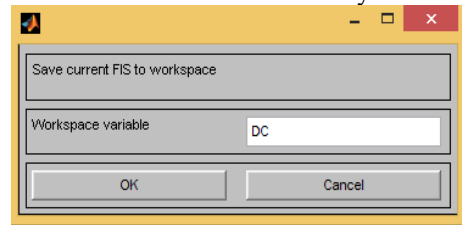


Fig.8 'Save to workspace as...' window

By saving to the workspace with a new name, we also rename the entire system. Our window will look like as shown in Fig.8.

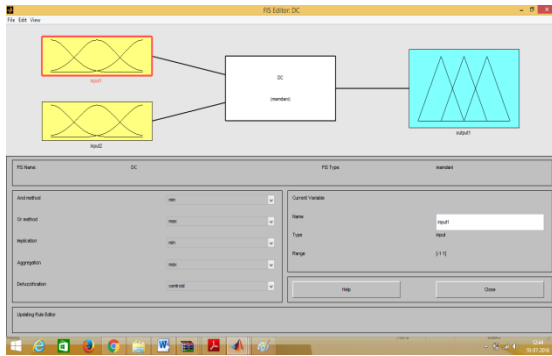


Fig.9 The Updated FIS Editor

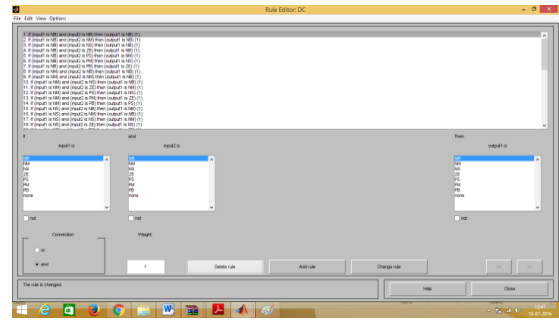


Fig.13 The Rule Editor

## 4.2 The Membership Function Editor

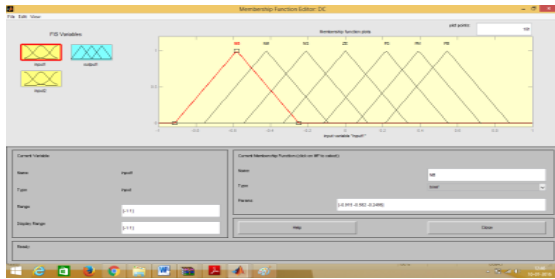


Fig. 10 The Membership Function Editor

	NB	NM	NS	ZE	PS	PM	PB
NB	NB	NB	NB	NB	NM	NS	ZE
NM	NB	NB	NB	NM	NS	ZE	PS
NS	NB	NB	NM	NS	ZE	PS	PM
ZE	NB	NM	NS	ZE	PS	PM	PB
PS	NM	NS	ZE	PS	PM	PB	PB
PM	NS	ZE	PS	PM	PB	PB	PB
PB	ZE	PS	PM	PB	PB	PB	PB

Fig.14 Fuzzy rules

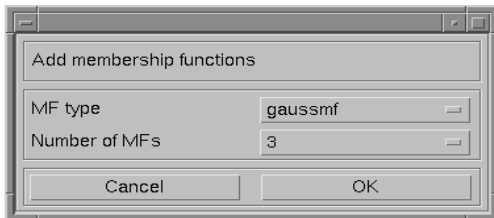


Fig.11 Add MFs... Window

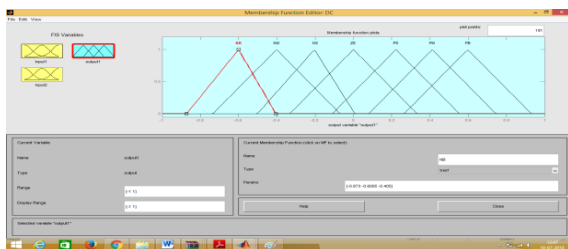


Fig.12 The Updated Membership Function Editor

## 4.3 The Rule Editor

## V.SIMULATION RESULTS

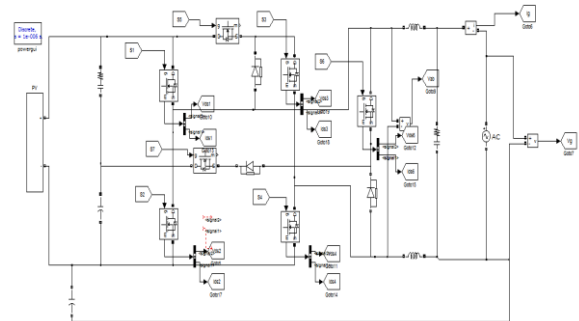


Figure 15: Simulink model of proposed system

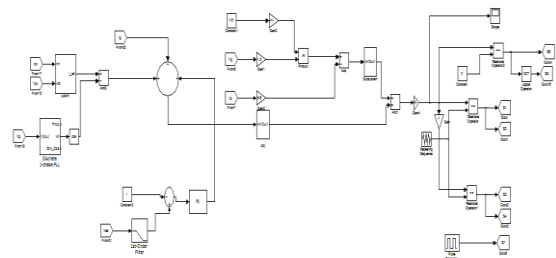


Figure 16: control diagram with PI controller

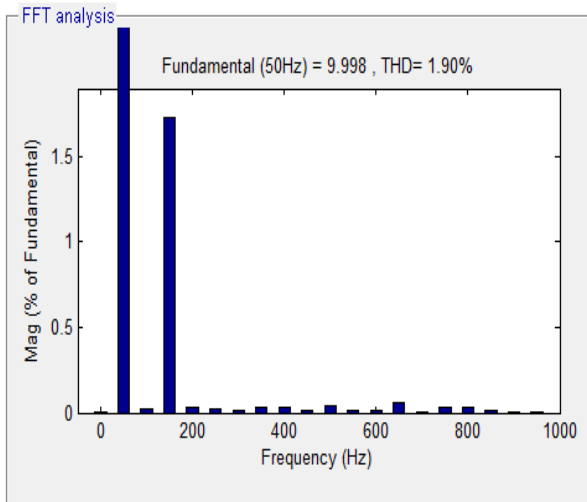


Figure 17: Total harmonic distortion of output current Using PI controller

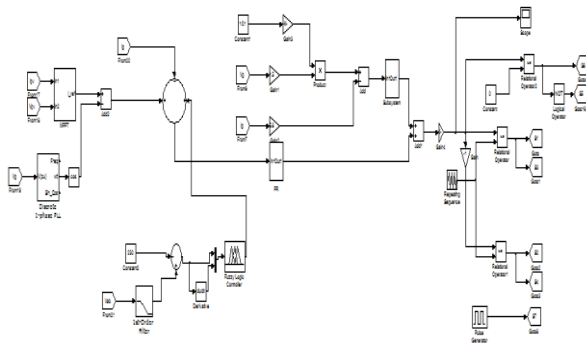


Figure 18: control diagram of proposed system

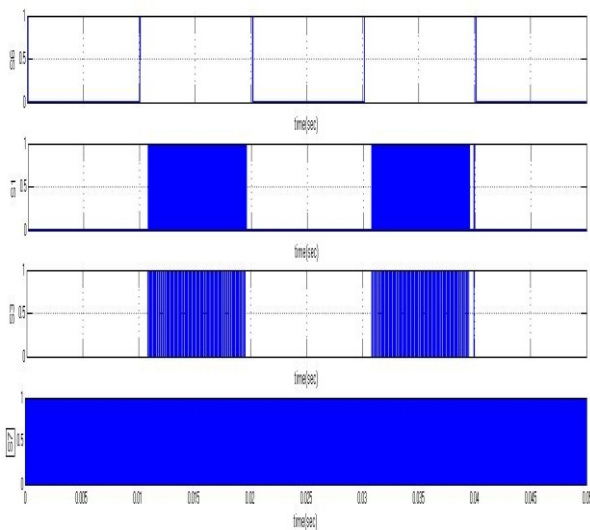


Figure 19: Gates pulses of switches S6, S1, S3 and S7

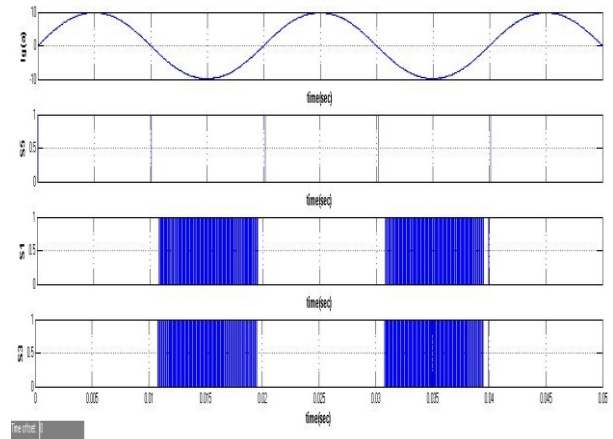


Figure 20: Grid current(Ig) and gate pulses for switches S6, S1 and S3

In order to verify the performance of the proposed topology and to compare with other topologies, The Simulink model of proposed model is given in Figure 17 and It is clear that the gate signals are in agreement with the theoretical and the gate drive voltages are kept constant at the desired level. It also can be observed from Figure 1 and Figure 20 that the gate signals G1 and G4 are well synchronized, while G7 is the contrary gate pulse of G1 and G4 with a small dead band.

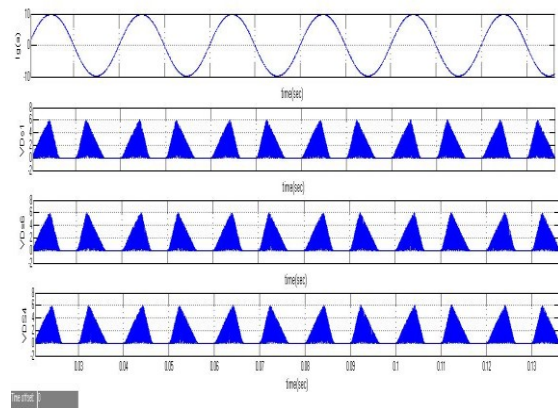


Figure 21: Drain to source voltage of different switches S1, S6 and S4

Figure 21 shows the drain-source voltage waveforms of the switches S1, S4, and S6. This shows that the switching voltages of the switches are half of the dc input voltage without any overstress. The partial expansion of Figure 21 is showing that the switches S1 and S4 almost share the dc-link voltage when they commute with high frequency.

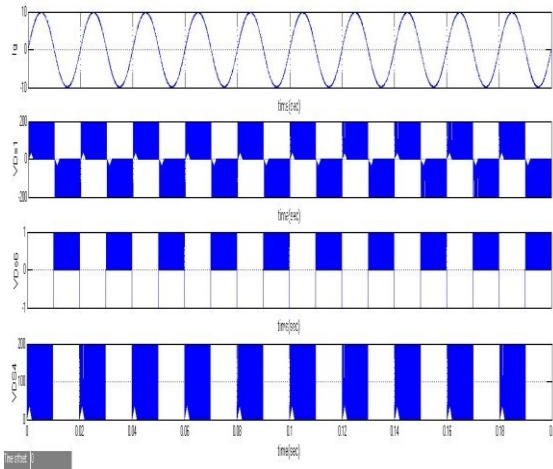


Figure 22: Grid current & switch voltages  $V_{DS1}$ ,  $V_{DS6}$  and  $V_{DS4}$

The partial expansion of Figure 22 is provided that the switches S1 and S4 almost share the dc-link voltage when they commute with high frequency. Therefore, the switching losses are minimized, and the results fulfill the theoretical analysis. The peak is same as grid peak current  $I_m$ .

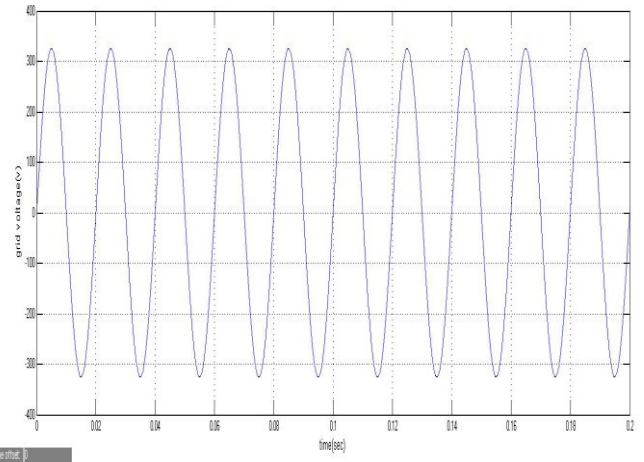


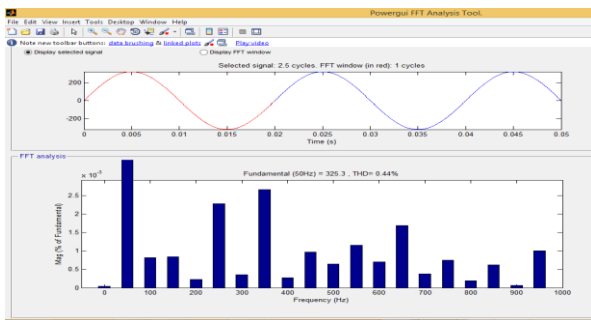
Figure 25 Grid voltage

## VI. CONCLUSION

In this project, a family of new efficient transformer less inverter for a grid-tied PV power generation system is presented using super junction MOSFETs as main power switches. The main advantages of the proposed topology are as follows. High efficiency over a wide load range is achieved by using MOSFETs and SiC diodes, CM voltage remains constant during all operation modes due to the added clamping branch, results low leakage current, like as isolated FB inverter, excellent DM characteristics are achieved with unipolar SPWM, and PWM dead time is not required for main power switches, results low distortion at output with fuzzy controller. Therefore, it can be concluded that the proposed inverter is very suitable for a single-phase grid-tied PV application.

## REFERENCES

- [1] M. Islam, S. Mekhilef, and M. Hasan, "Single phase transformerless inverter topologies for grid-tied photovoltaic system: A review," *Renewable and Sustainable Energy Reviews*, vol. 45, pp. 69-86, 2015.
- [2] I. Patrao, E. Figueres, F. González-Espín, and G. Garcera, "Transformerless topologies for grid-connected single-phase photovoltaic inverters," *Renewable and Sustainable Energy Reviews*, vol. 15, pp. 3423-3431, 2011.
- [3] Z. Li, S. Kai, F. Lanlan, W. Hongfei, and X. Yan, "A Family of Neutral Point Clamped Full-Bridge Topologies for Transformer Photovoltaic Grid-Tied Inverters," *IEEE Transactions on Power Electronics*, vol. 28, pp. 730-739, 2013.
- [4] M. Islam and S. Mekhilef, "H6-type transformerless single-phase inverter for grid-tied photovoltaic system," *IET Power Electronics*, vol. 8, pp. 636-644, 2015.



FiFig 23 Total harmonic distortion of output voltage with Fuzzy controller

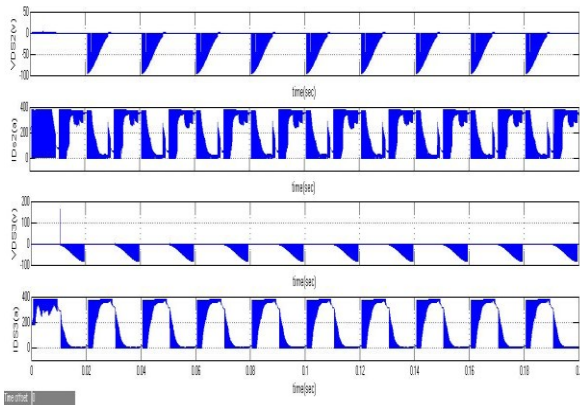


Fig.7.24: Voltages and currents of Switch S2 and S3

[5] J. Baojian, W. Jianhua, and Z. Jianfeng, "High-Efficiency Single Phase Transformerless PV H6 Inverter With Hybrid Modulation Method," IEEE Transactions on Industrial Electronics, vol. 60, pp. 2104-2115, 2013.

[6] D. Barater, G. Buticchi, E. Lorenzani, and C. Concari, "Active Common-Mode Filter for Ground Leakage Current Reduction in Grid-Connected PV Converters Operating With Arbitrary Power Factor," IEEE Transactions on Industrial Electronics, vol. 61, pp. 3940-3950, 2014.

[7] T. Kerekes, R. Teodorescu, P. Rodriguez, G. Vazquez, and E. Aldabas, "A New High-Efficiency Single-Phase Transformerless PV Inverter Topology," IEEE Transactions on Industrial Electronics, vol. 58, pp. 184-191, 2011.

[8] G. Bin, J. Dominic, L. Jih-Sheng, C. Chien-Liang, T. LaBella, and C. Baifeng, "High Reliability and Efficiency Single-Phase Transformerless Inverter for Grid-Connected Photovoltaic Systems," IEEE Transactions on Power Electronics, vol. 28, pp. 2235-2245, 2013. [9] Y. Bo, L. Wuhua, G. Yunjie, C. Wenfeng, and H. Xiangning, "Improved Transformerless Inverter With Common-Mode Leakage Current Elimination for a Photovoltaic Grid-Connected Power System," IEEE Transactions on Power Electronics, vol. 27, pp. 752-762, 2012.

[10] H. Guofeng, X. Dehong, and C. Min, "A Novel Control Strategy of Suppressing DC Current Injection to the Grid for Single-Phase PV Inverter," IEEE Transactions on Power Electronics, vol. 30, pp. 1266-1274, 2015.